C S

Multiple Olfactory Activity in the Human Neocortex Identified by Magnetic Source Imaging

Birgit Kettenmann, Cornelia Hummel[1], Hermann Stefan[1] and Gerd Kobal

Department of Experimental and Clinical Pharmacology and Toxicology, Krankenhausstrasse 9 and [1]Department of Neurology, Schwabachanlage 10, University of Erlangen-Nürnberg, D-91054 Erlangen, Germany

Correspondence to be sent to: Dr Birgit Kettenmann, Department of Experimental and Clinical Pharmacology and Toxicology, Krankenhausstrasse 9, D-91054 Erlangen, Germany

Abstract

To date, cortical regions activated by olfactory stimulation have not been identified precisely in humans. In this study we used magnetic source imaging to localize neuronal activity following olfactory stimulation with two odorants, hydrogen sulphide and vanillin. Peak latencies of the olfactory event-related magnetic fields corresponded to the ascending and descending slopes of the major deflections of the olfactory event-related potentials (OERP). At these latencies we obtained consistent activation of the anterior–central parts of the insula (agranular–periallocortical and dysgranular regions), the parainsular cortex and the superior temporal sulcus. No reproducible equivalent current dipoles were found in other brain areas, including the orbitofrontal cortex. For the first time, brain areas were identified that generate most components of olfactory bioresponses (OERPs) in humans. **Chem. Senses 22: 493–502, 1997.**

Introduction

The cerebral representation of odour perception in man is poorly understood compared with other sensory modalities such as hearing, vision or touch. This may partly result from the lack of appropriate instruments for specific stimulation of chemosensors that makes investigation of this system extremely difficult. Primary olfactory structures, namely the olfactory bulb, olfactory tract and piriform cortex, that have been studied in animal experiments are also recognizable in humans (Price, 1990). Little is known of neocortical regions that might be involved in processing of olfactory information. Findings in patients with brain lesions indicate that for perception of odours the temporal lobe is of critical importance (Eichenbaum *et al.*, 1983; Eskenazi, 1986).

Recent progress in neuronal imaging has allowed the study of the functional topography of the olfactory system with detailed temporal and spatial resolution. Positron emission tomography (PET) showed for the first time that, in addition to a bilateral increase of cerebral blood flow (CBF) in the piriform cortex, the insular cortex and the right orbitofrontal cortex were also activated by odorous stimulation (Zatorre *et al.*, 1992). Another experiment using functional magnetic resonance imaging (fMRI) also showed a significant bilateral increase in CBF in the piriform cortex and the orbitofrontal cortex (Koizuka *et al.*, 1994). The major disadvantage of these two imaging techniques is their low temporal resolution. Time windows are >1 s for fMRI; for PET they approach 1 min. By using olfactory event-related potentials (Finkenzeller, 1966; Allison and

Goff, 1967; Kobal and Plattig, 1978; Kobal, 1981; Kobal and Hummel, 1988; for review see Kobal and Hummel, 1991) it has become possible to non-invasively record the activity of cortical neurons in fractions of a second. Recently, magnetic source imaging (MSI) having the same time resolution has been used to identify those brain areas generating the P2 component of the olfactory evoked potential (Kettenmann *et al.*, 1996).

The general goal of magnetoencephalography (MEG) used for MSI is to localize magnetic fields measured at the surface of the scalp (Cohen, 1972). These magnetic fields are generated by a number of cerebral neurons electrically active at the same time. Assuming that the human head is a spherical volume conductor (Abraham-Fuchs *et al.*, 1988) and electrical neuronal activity has the property of a current dipole characterized by an electric field and an orthogonal magnetic field, it is possible to calculate the location, orientation and strength of the current source that generates the magnetic field measured at the surface of the sphere (Williamson and Kaufman, 1981; Romani *et al.*, 1982). There are two general problems within the technique of MSI: firstly, because it is not possible to deduce from a given isomagnetic field map the number of underlying dipoles (inverse problem; Helmholtz, 1853), it is thought that a recorded field pattern at the surface of a human skull may be generated by several dipoles. Secondly, a radial dipole does not produce a magnetic field that can be measured with the usual positioning of the magnetometer (i.e. the coils are arranged parallel to the surface of the skull). This type of dipole is 'silent' and cannot be localized.

Once a magnetic field is measured, a plausible dipole position is estimated. Then a nonlinear fit-strategy, such as a Marquardt (1963) or Powell (1964) algorithm, is applied to enhance the estimation. By this procedure the location, strength and orientation of the determined dipole is iteratively changed in such a way that the magnetic field produced by this calculated dipole more and more precisely corresponds to the dipole measured by the magnetometer. The statistical procedure is based on the method of 'least squares'. The result of these calculations is then called the 'equivalent current dipole' ECD. An extensive description of this data analysis can be found elsewhere (Scholz and Oppel, 1992). The accuracy of the localization strongly depends on the signal-to-noise ratio (SNR) of the measured data and decreases with increasing depth of the dipole within the sphere. The localization is better for a dipole centred below the array of coils than below the outer parts of the array. Errors of this type can only be estimated by using simulations (Barth, 1986; Janday, 1987; Hari, 1988; Meijs, 1988).

By linking the coordinates of magnetically defined ECDs to the anatomical MRI data (Stefan *et al.*, 1990), it is then possible to visualize the location of activated areas in the individual subject's brain and to check them for their anatomical and physiological plausibility. All these techniques used for the interpretation of measured magnetic fields help to localize cortical neuronal activity reliably and help obtain a functional topography (for review see Williamson and Kaufman, 1981, 1989; Romani *et al.*, 1982; Hari and Illmoniemi, 1986; Romani and Narici, 1986; Hoke, 1988; Hari and Lounasmaa, 1989).

The reliability of estimation is further influenced by external errors such as magnetic noise caused by electric devices, artifacts caused by movements of the subjects, or by electric activity of the heart (Abraham-Fuchs *et al.*, 1988; Hansen *et al.*, 1988; for review see Hämäläinen *et al.*, 1993).

Employing a whole-head neuromagnetometer at the Low Temperature Laboratory in Helsinki, Finland, Kettenmann *et al.* (1996) found bilateral activation in the superior temporal sulcus ~700 ms after stimulation with the odorants vanillin and hydrogen sulphide. These two substances were chosen because they are primarily olfactory, i.e. they have no activation of the trigeminal nerve and therefore fulfil the prerequisites for studying the sense of smell (Beidler and Tucker, 1956; Doty *et al.*, 1978; Silver *et al.*, 1986; Kobal and Hummel, 1991; Hummel and Kobal, 1992).

One aim of this study was to confirm earlier results obtained with a whole-head magnetometer (Kettenmann *et al.*, 1996) by using a planar 37-channel sensor array (Erlangen, Krenikon™), and more importantly, to identify the neuronal generators underlying the components of the olfactory event-related potentials 200–700 ms after stimulus onset.

Materials and methods

Subjects

Ten healthy volunteers participated in the experiments (five male and five female, 20–40 years of age, mean age 28 years). They were trained to avoid eye blinks or other movement artifacts. Since respiratory airflow in the nose might have quantitatively influenced the stimuli, subjects performed a special breathing technique (velopharyngeal closure; Kobal 1985).

The study was conducted in accordance with the revised version of the Helsinki/Hong Kong declaration and was approved by the Ethics Committee of the University of Erlangen-Nürnberg.

Stimulation

For olfactory stimulation, an apparatus was employed which delivered the stimulants without altering the mechanical or thermal conditions at the mucosa (Kobal, 1985; Kobal and Hummel, 1988). This monomodal olfactory stimulation is achieved by mixing pulses of the odorants in a constantly flowing airstream (total flow rate 140 ml/s) with controlled temperature and humidity (36.5°C, 80% relative humidity). Stimuli were applied non-synchronously to breathing. The vanillin concentration was determined prior to the experiments using gas chromatography. In the case of hydrogen sulphide, predefined concentrations in pressure gas cylinders (22 p.p.m.) were used. Before each session the olfactometer was calibrated and the concentration was calculated by the flow rates of an additional dilution line (air) and the prediluted odorant. For more details on the olfactometer see Kobal (1985) and Kobal and Hummel (1988).

The olfactometer was especially designed for this experiment. Twelve separate temperature controlled Teflon tubes were fed through a grid with 3 × 3 cm holes in the wall of the magnetically shielded room. This did not alter the quality of shielding as controlled by frequency distribution of the noise. All parts of the olfactometer consisted of non-magnetic materials such as Teflon, silicon, Plexiglas, glass, gas and water. Even at a distance of 5 m between the outlet of the olfactometer and the solenoid valves, the olfactometer can provide a steep increase of odour pulses as verified by measuring CO_2 pulses with a thermistor (for more details see Kobal, 1985). Subjects were comfortably seated in a magnetically shielded, ventilated chamber which could be monitored by means of a video system. White noise (~60 dB SPL) applied to both ears was used to mask the switching clicks of the stimulator. The sound was transferred via air conduction through two hollow plastic tubes which were used as a connection between the acoustic amplifier outside the shielded room and the subjects' ears. Each subject participated in six experimental sessions (three experimental sessions for one nostril) on each of four experimental days. In one experimental day either one of the two substances hydrogen sulphide (0.8 ppm) or vanillin (2.1 ppm) was tested with the sensor array positioned over one hemisphere. Sites of sensor location (left/right hemisphere MEG recording) and application of both odorants were randomized across all participating subjects. During each of the three sessions (performed for each nostril) 30 stimuli of the same odour were applied by way of Teflon tubing (6 cm length, 2 mm inner diameter). To avoid habituation, a stimulus duration of 200 ms and an interstimulus interval of 40 s was used so that there was no residual odorant left in the tubings. Additionally, the three sessions performed for one nostril were separated by breaks of 10 min. Subsequently, data were averaged across these sessions if the head position of the subject had not changed (controlled by a laser motion detector).

Olfactory event-related potentials (OERPs)

For comparison with MEG recordings, OERPs were obtained from the vertex (Cz/A1). They were used to facilitate interpretation of the magnetic responses.

Olfactory event-related magnetic fields (OERMFs)

OERMFs were obtained by means of a biomagnetic system (Siemens Krenikon™) with 37 first-order gradiometers (baseline 7 cm) in a circular arrangement of 19 cm diameter (Hoenig *et al.*, 1991). It was possible to obtain isocontour plots from the region of interest without repositioning the sensors. Both EEG and MEG were recorded at a sampling rate of 500 Hz, a bandpass filter 0.1–70 Hz and an offline 30 Hz low-pass digital filter. The source analyses were based on signals averaged from artifact free records ($30 < n < 90$).

For data evaluation we used a map correlation ≥0.92 (defined as coefficient of correlation). We used an interval length with a minimum of 0.006 s. The upper and lower limits for the strength of the estimated source were defined as > 0.007 < 0.03 mA·mm (Abraham-Fuchs *et al.*, 1996).

An upper limit for the rate of change of the source strength was defined (factor <10). The acceptable localization error was set to a maximum of 20 mm; it was defined as the area in which the equivalent current dipole had its possible location.

A magnetic field was called consistent if it lasted for a minimum time period of 10 ms. The time of best fit (TOBF) for one ECD represents the time point where the isofield map of this special ECD shows its best 'map correlation'. That is, at this TOBF the measured map of the ECD has the best correlation with the theoretically calculated map, the

smallest localization error and the highest SNR.This does not mean that the neuronal source is only active at this point in time. It can already start being active several milliseconds before and last longer than this TOBF, but dependent on the actual situation, it can be masked by additional neuronal activity from other sources. Therefore, the TOBF of the ECDs must not be considered a measure of the onset of neuronal activity. The field patterns were called reproducible when the ECDs could be localized with the predefined validation criteria at about the same TOBF in about the same anatomical structure.

The SNR of the data determines the accuracy in biomagnetic source reconstruction. In order to increase the SNR we used the averaging procedure (Abraham-Fuchs *et al.*, 1990). A vertical electro-oculogram was used to detect signals generated by eye blinks or movements. Records contaminated with EOG deflections >200 μV were rejected. The noise level of the pre-trigger period of the averaged session was estimated and the mean values used as a baseline. The noise level of all 64 measurements ranged from 0.00003 to 0.000488 pT with a mean value of 0.000222 pT and a standard deviation of 0.000128 pT. The signals of the ECDs were ~8–10 times higher than the mean values of the noise. No average across experimental days or after repositioning was calculated.

To provide accurate images of individual brain anatomy, MRI was employed. For the alignment of the functional MEG information with the MRI, a head coordinate system was created for each subject and defined by the nasion and two preauricular points. Water-filled pellets (0.3 mm diameter) were attached to the subject's skin and, subsequently, their MRI coordinates were transformed into the coordinate system of the MSI data. To deduce the positioning of the subjects' head with respect to the sensor array after head positioning, the three landmarks were digitized with a 3-D scanner (Isotrak, Polhemus Navigation Sciences, Colchester, VT) and subsequently aligned with the coordinate system received from the MRI. This method of alignment presupposes that the subject is not moving during the measurement, since changes of head position cannot be corrected. However, they were monitored by a laser motion detector. To minimize the possibility of movement, the head was stabilized with a vacuum pillow.

Control measurements were carried out to exclude contamination of the measured signals by tactile or auditory artifacts, by localizing the corresponding ECDs of these sensory systems and comparing them with the ECDs found after chemical stimulation. Odorless stimuli delivered to the nostrils by the especially designed olfactometer did not produce any activity as assessed by means of MEG or EEG measurements.

Statistical evaluation by means of a chi-square test was carried out to compare the frequency of the three different ECDs dependent on the side of stimulation and the odorant that was used.

Results

The signal quality of the evoked responses was sufficient for source localization in 8/10 subjects. Consistent magnetic fields were identified in both hemispheres following stimulation of each nostril. In 60% of measurements, reproducible dipolar field patterns were obtained 226–380 ms after stimulus onset, preceding or following the first major positive electrical deflection of the event-related potential (P1). This equivalent current dipole was named ECD I. In 44% of the measurements a reproducible dipolar distribution was obtained 306–486 ms after stimulus onset, corresponding to the ascending or descending slope of the N1 component, which was named ECD II. In the left hemisphere, this dipole was not identifiable in any of the subjects after stimulation with hydrogen sulphide. It was identifiable only in the right hemisphere in 36% of the measurements. The most stable dipolar field pattern appeared 518–730 ms after stimulus onset (in 66% of the measurements; ECD III), corresponding to the P2 component of the electrical response (Figure 1).

Figure 1 shows averaged OERMFS recorded from one subject over the right hemisphere after stimulation of the right nostril with vanillin. In this case ECDs with best fits were obtained at 324 ms (ECD I), 434 ms (ECD II) and 568 ms (ECD III) after stimulus onset. Orientation of the sources indicated current flow towards central/parietal regions for ECD I and ECD III. For ECD II, current flow pointed into the opposite direction consistently with the polarity of the peaks of the OERPs. The orientations towards parietal regions might explain maximal electrical responses at parietal leads for the components P1 (268–388 ms), N1 (366–474 ms) and P2 (472–749 ms) of the olfactory event-related potentials which have been demonstrated in a series of previous studies (Hummel and Kobal, 1992; Kobal *et al.*, 1992).

The estimated ECDs I, II and III of the measurement

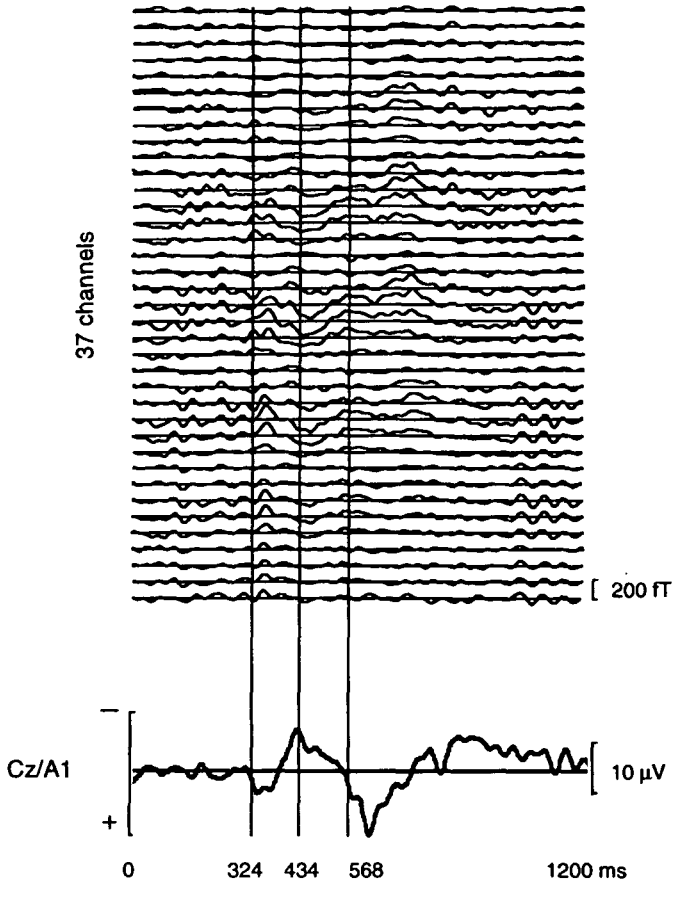

Figure 1 Example from one subject: 37 channel magnetoencephalographical recordings from the right hemisphere after right nostril stimulation with vanillin. The lines indicate the latencies (324, 434 and 568 ms) of the magnetic fields used for calculating the topographic isocontour plot of the three ECDs. We evaluated the magnetic responses in the time range from beginning of stimulation up to 1200 ms after stimulus onset. Since all 37 channels were taken into account, it was possible there were channels showing magnetic fields with high amplitudes but producing a monopolar field pattern with no valid localization. In contrast, there are magnetic fields with smaller amplitudes but producing a dipolar field pattern and resulting in a valid localization. For comparison the simultaneously recorded OERP (lead Cz/A1) is shown at the bottom with the same temporal resolution as the magnetic field recordings. It was only used as orientational time marker.

shown in Figure 1 are superimposed on anatomical MRI of the same subject in Figure 2. In five subjects and 14% of all the measurements, all three ECDs could be identified during one session. Similar to the examples shown in Figures 1 and 2, in all cases where ECD I was identified, it was localized in the area between the superior temporal plane and the parainsular cortex. In seven out of eight subjects a generator was significantly localized in the left hemisphere after stimulation of the left nostril with vanillin ($\chi^2 = 4.5$; df = 1; $P = 0.034$). ECD II was localized in the anterior–central parts of the insula. In seven out of eight subjects this generator was significantly localized in the right hemisphere after stimulation of the right nostril with vanillin ($\chi^2 = 4.5$; df = 1; $P = 0.034$). ECD III was obtained in the superior temporal sulcus. In seven out of eight subjects this generator was localized in the left hemisphere after stimulation of the left nostril with hydrogen sulphide ($\chi^2 = 4.5$; df = 1; $P = 0.034$). In none of these measurements was ECD II obtained in the left hemisphere after stimulation with hydrogen sulphide.

Interindividually, spatial differences of localization sites for one type of ECD were less than 20 mm. Intraindividually, the angle of orientation varied between 10 and 30° in all three dimensions; the dipole strength varied between 0.009 to 0.03 mA·mm.

Discussion

Using the odorants vanillin and hydrogen sulphide for stimulation, which we think more specifically activate the sense of smell than those odorants used by *Zatorre and Koizuka*, the OERFs were localized to specific neocortical areas. During the latent period of the OERP (200–800 ms), areas between the superior temporal plane, the parainsular cortex, anterior–central parts of the insula and the superior temporal sulcus were active. These electro(magneto)physiological data confirm the suggestion of direct connection between primary olfactory areas and the insular cortex (Mesulam and Mufson, 1982). Experiments in animals using axonal tracers consistently demonstrate inputs from the primary olfactory cortical areas to the ventral agranular insular area (Clugnet and Price, 1987; Carmichael *et al.*, 1994). The results of the present study describing activity in the superior temporal sulcus (ECD III) also confirm findings of our earlier work using a whole-head neuromagnetometer (Kettenmann *et al.*, 1996). These data indicate for the first time the activation of the superior temporal sulcus after olfactory stimulation in man. This is supported by the known anatomical connection between the inferior orbitofrontal areas that receive input from specific olfactory structures, i.e. the primary olfactory cortex and the superior temporal sulcus in primates (Carmichael and Price, 1995). With one exception (see below), both the location and the orientation of the dipoles exhibit good reproducibility. Hence, both odorants appeared to activate similar cortical areas.

The data also showed bilateral neocortical activation after

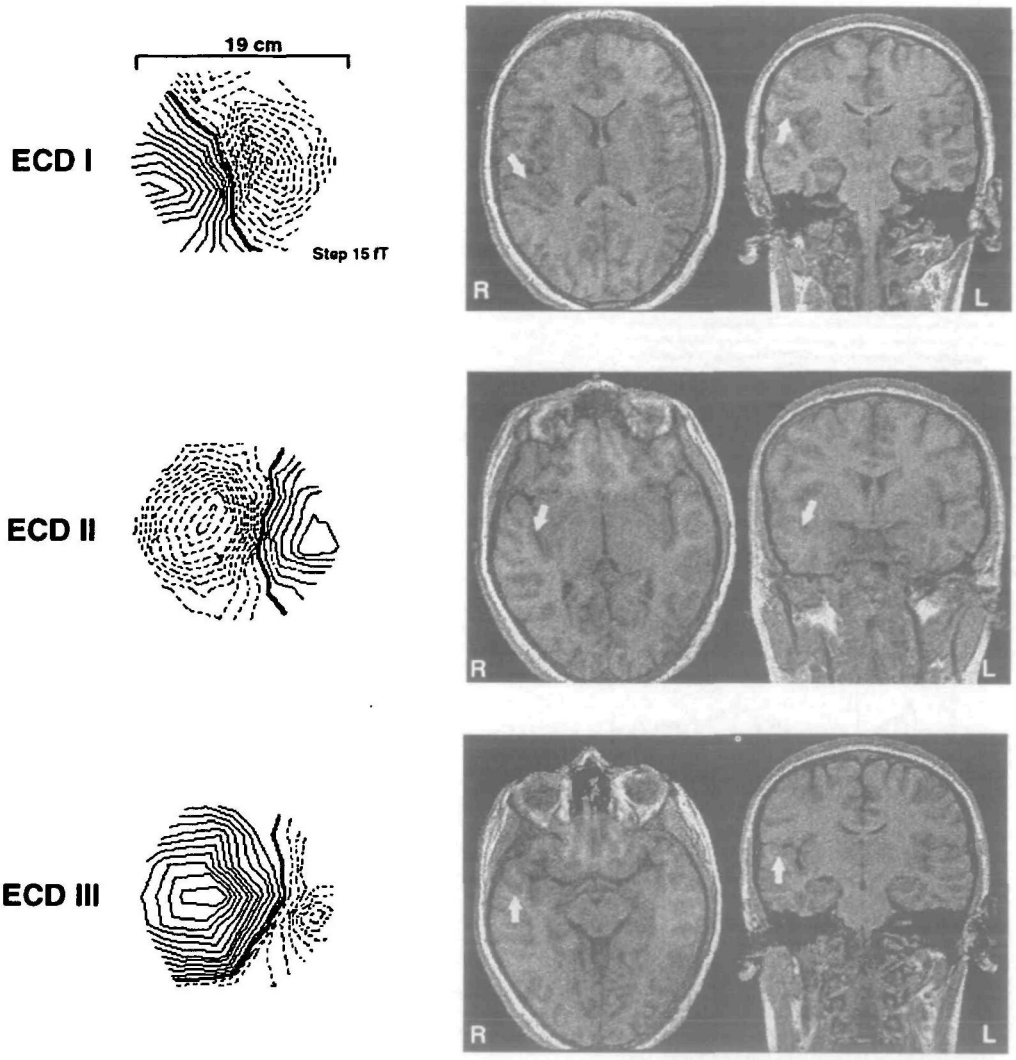

ECD	latency (ms)	coordinates (mm)			orientation (mA*mm)		
		x	y	z	qx	qy	qz
I	324	-7	-15	-55	-0.333	0.941	0.065
II	434	11	-22	-80	-0.636	-0.768	-0.073
III	568	-6	-33	-66	0.738	0.528	0.420
sphere origin (r = 71 mm)		-1	-5	-114			

All other data are available from the authors

Figure 2 Example from one subject (same as in Figure 1): localization of neuronal activity after vanillin stimulation of the right nostril. All three ECDs (ECD I–III) are shown. The arrows indicate activated cortical regions in the axial and coronal views; the arrow size corresponds to the size of the dipole vector. The isocontour plots represent the magnetic field distribution measured at a certain time. They reflect the geometry of the 37 sensors. With respect to the coordinate system of the sphere model and the coordinate system of the sensor region (below), the dipole orientation in the sphere model was calculated. ECD I was localized between the superior temporal plane and the parainsular cortex (map correlation, 0.96; dipole error, 14.0 mm). The cortical area activated after 434 ms (ECD II) was located in the anterior–central part of the insula (map correlation, 0.98; dipole error, 11.0 mm); after 568 ms (ECD III) neuronal activity in the superior temporal sulcus was obtained (map correlation, 0.96; dipole error, 18.3 mm). Bottom left: orientation and coordinates of the three ECDs shown above with respect to the sphere origin. Bottom right: positioning of the sensor array and the model sphere used for calculation. The sensors were placed over the temporal lobe of the right hemisphere.

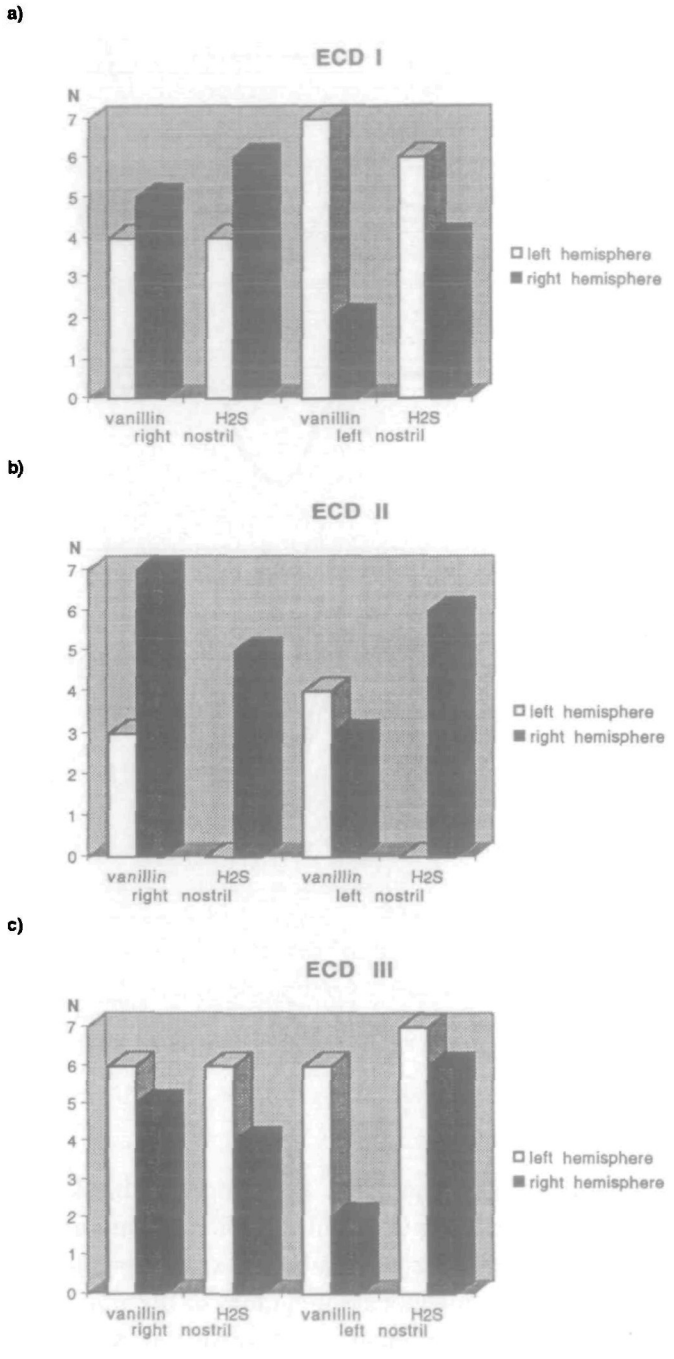

Figure 3 Frequency distribution of the ECDs: the bar chart indicates that the three ECDs differed in relation to the side of stimulation, the recording site and the two odorants (vanillin and hydrogen sulphide) used. The frequency of the localization of ECD I in the left hemisphere after stimulation of the left nostril with vanillin was statistically significant. The frequency of the localization of ECDII in the right hemisphere after stimulation of the right nostril with vanillin was statistically significant as well as ECD III in the left hemisphere after stimulation of the left nostril with hydrogen sulphide.

lateralized stimulation, in contrast to other evidence that suggests olfactory input is primarily processed ipsilaterally to the stimulated nostril (Gordon and Sperry, 1969; Youngentoub *et al.*, 1982). In animal studies, it was demonstrated that there are bilateral connections between the anterior olfactory nucleus, the anterior part of the piriform cortex and the neocortical areas. The fibres cross in the anterior commissure and are distributed equally in both hemispheres (Price, 1990). We were not able to identify the ECD II in the left hemisphere after stimulation with hydrogen sulphide. This might indicate the coding of qualitative differences between hydrogen sulphide and vanillin. Although this hypothesis must be tested extensively using a larger range of odorants, it has already been demonstrated that amplitudes and latencies of OERPs elicited by vanillin and hydrogen sulphide were correlated with their hedonic properties (Kobal *et al.*, 1992). Responses to hydrogen sulphide had significantly shorter latencies and smaller amplitudes after stimulation of the left nostril than responses after stimulation of the right nostril. In contrast, latencies were longer when the left nostril was stimulated with vanillin and N1/P2 amplitudes were significantly larger when compared with the responses after stimulation of the other nostril. This finding was reproduced in another experiment where subjective estimates of the odorants showed that after stimulation of the left nostril, the more pleasant the perception of the odor, the larger were the amplitudes and the longer were the latencies (Kobal *et al.*, 1989). In the light of the results of the present study this could mean that different cortical areas were activated after stimulation with odorants of different hedonic properties. There is also evidence for lateralization of hedonic information from clinical studies. Pleasant emotions seem to be processed predominantly by the left hemisphere, whereas unpleasant emotions appear to be handled by the right hemisphere (Dimond *et al.*, 1976; Davidson, 1984). The missing ECD II in the left insular cortex following hydrogen sulphide stimulation might justify the speculation that the observed differences in the responses to vanillin and hydrogen sulphide originate in the asymmetrical activation of the insular region (Figure 4). This does not yet explain why the differences in the OEP could only be observed when left and right nostril stimulation was compared.

Another indication for lateralization in the olfactory system was found by Hummel *et al.* (1995), investigating patients suffering from temporal lobe epilepsy. When olfactory stimuli were presented ipsilaterally to the epileptic focus, peak latencies of the OERP were prolonged in comparison with OERPs obtained after contralateral stimulation. Additionally, the topographical distribution

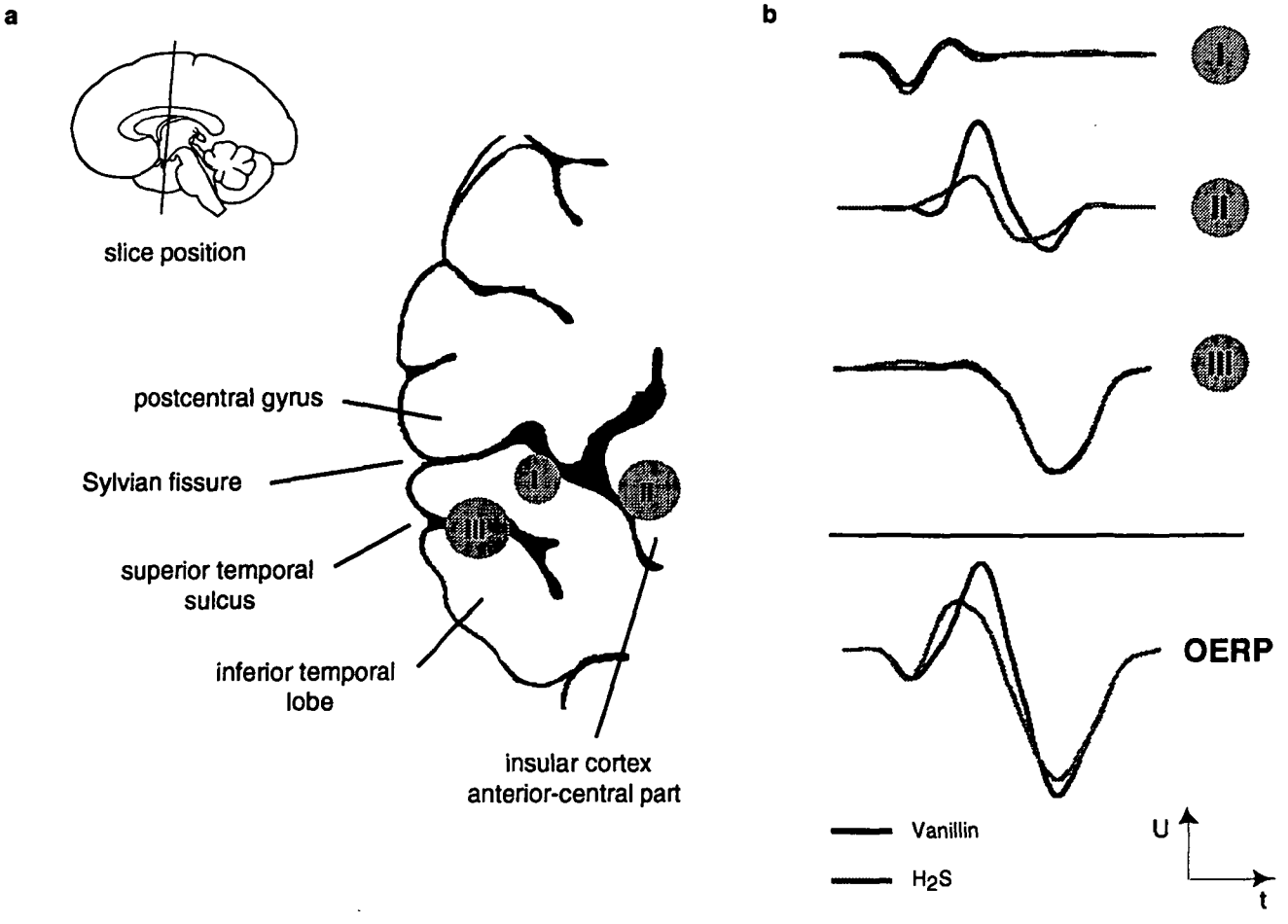

Figure 4 Hypothetical explanation for shorter latencies and smaller amplitudes of the N1 component in the OERP after stimulation with H_2S (dashed lines) compared with vanillin (solid lines) stimulation. The two lines each for ECDI, ECD II and ECD III in **b** show the theoretical electrical activity arising from different populations of neurons indicated in **a**. ECD II shows two different patterns of activation for the two stimuli in the anterior–central part of the insular cortex. The OERP reflects the summated electrical activity of the three cortical areas (ECD I–III). The maximum amplitude of the OERP is higher and the latency is longer when ECD II is very active (i.e. after vanillin stimulation), compared with a lower amplitude and a shorter latency of OERP if the activity of ECD II is weak or not present at all (i.e. after H_2S stimulation).

of the P2 component changed in patients with right-sided foci. In these patients the amplitude of P2 was maximal at Cz, whereas in previous studies in normal subjects, maximal P2 amplitudes were always obtained at Pz (Hummel *et al.*, 1992; Kobal *et al.*, 1992; Livermore *et al.*, 1992).

Olfactory dysfunction can produce severe impairment in the quality of life. Infections (e.g. postviral anosmia), degeneration (e.g. hyposmia in Alzheimer's and Parkinson's disease) or a tumour affecting the olfactory bulb (Murphy, 1987) are difficult to treat. In addition, the sense of smell plays a role in complex and controversial discussed disorders, such as idiopathic environmental intolerance (IEI) (T. Hummel *et al.*, submitted for publication). The underlying pathology might result from change in olfactory cortical function. Functional topography of the brain might be studied using the technique of MSI in disease states.

To summarize, for the first time, brain areas were identified that generate components of human olfactory bioresponses (OERPs and OERFs). Our results suggest that apart from the known primary olfactory areas, these neocortical areas are specifically involved in the processing of olfactory information in humans.

ACKNOWLEDGEMENTS

This research was supported by DFG grant Ko812/5-1. We thank Dr Elisabeth Pauli, Department of Neurology, University of Erlangen-Nürnberg, for performing the statistical analysis of the data.

REFERENCES

Abraham–Fuchs, K., Schneider, S. and Reichenberger, H. (1988) MCG inverse solution: influence of coil size, grid size, number of coils and SNR. *IEEE Trans Biom. Engng*, **BE-35**, 573–576.

Abraham-Fuchs, K., Härer, W., Schneider, S. and Stefan, H. (1990) Pattern recognition in biomagnetic signals by spatiotemporal correlation and application to the localization of propagating neuronal activity. *Med. Biol. Engng Computat.*, **28**, 398–406.

Abraham-Fuchs, K., Schneider, S. and Stefan, H. (1996) Principles of magnetoencephalography. In Pawlik, K., Stefan, H. (eds.) *Focus Localization*. Liega Selbstverlag, Thomas Wiese, Berlin.

Allison, T. and Goff, W.R. (1967) Human cerebral evoked responses to odorous stimuli. *Electroenceph. Clin. Neurophysiol.*, **23**, 558–560.

Barth, D.S., Sutherling, W., Broffman, J. and Beatty, J. (1986) Magnetic localization of dipolar current source implanted in a sphere and a human cranium. *Electroenceph. Clin. Neurophysiol.*, **63**, 260–73.

Beidler, L.M. and Tucker, D. (1956) Olfactory and trigeminal nerve responses to odors. *Fed. Proc.*, **15**, 14–21.

Carmichael, S.T. and Price, J.L. (1995) Sensory and premotor connections of the orbital and medial prefrontal cortex. *J. Comp. Neurol.*, **363**, 642–664..

Carmichael, S.T., Clugnet, M.-C. and Price, J.L. (1994) Central olfactory connections in the macaque monkey. *J. Comp. Neurol.*, **346**, 403–434.

Clugnet, M.-C. and Price, J.L. (1987) Olfactory input to the prefrontal cortex in the rat. *Ann. NY Acad. Sci.*, **510**, 231–235.

Cohen, D. (1972) Magnetoencephalography: detection of the brain's electrical activity with a superconducting magnetometer. *Science*, **175**, 664–666.

Davidson, R.J. (1984) Affect, cognition and hemispheric specialization. In Izard, C.E., Kagan, J. and Zajonc, R. (eds), *Physological Correlates of Human Behavior*. London, Academic Press.

Dimond, S.J., Farrington, L. and Johnson, P. (1976) Differing emotional responses from right and left hemispheres. *Nature*, **261**, 690–692.

Doty, R.L., Brugger, W.P.E. v, Jurs, P.C. Orndorff, M.A., Snyder, P.J. and Lowry, L.D. (1978) Intranasal trigeminal stimulation from odorous volatiles: psychometric responses from anosmics and normal humans. *Physiol. Behav.*, **20**, 175–185.

Eichenbaum, H., Morton, T.H., Potter, H. and Corkin, S. (1983) Selective olfactory deficits in case H.M. *Brain*, **106**, 459–472.

Eskenazi, B. (1986) Odor perception in temporal lobe epilepsy patients with and without temporal lobectomy. *Neuropsychologia*, **24**, 553–562.

Finkenzeller, P. (1966) Gemittelte EEG—Potentiale bei olfaktorischer Reizung. *Pflügers Arch.*, **292**, 76–80.

Gordon, H.W. and Sperry, R.W. (1969) Lateralization of olfactory perception in the surgically separated hemispheres of man. *Neuropsychologia*, **7**, 11–120.

Hämäläinen, M., Hari, R., Ilmoniemi, R.J., Knuutila, J. and Lounasmaa, O. (1993) Magnetoencephalography—theory, instrumentation, and applications to noninvasive studies of the working human brain. *Rev. Modern Phys.*, **65**, 413–497.

Hansen, J.S., Ko, H.W., Fisher, R.S. and Litt, B. (1988) Practical limits on the biomagnetic inverse process determined from *in vitro* measurements in spherical conducting volumes. *Phys. Med. Biol.*, **33**, 105–111.

Hari, R. and Ilmoniemi, R.J. (1986) Cerebral magnetic fields. *CRC Crit. Rev. Biomed. Engng*, **14**, 93–126.

Hari, R. and Lounasmaa, O.V. (1989) Recording and interpretation of cerebral magnetic fields. *Science*, **244**, 432–436.

Hari, R., Joutsiniemi, S.L. and Sarvas, J. (1988) Spatial resolution of neuromagnetic records: theoretical calculations in a spherical model. *EEG Clin. Neurophysiol.*, **71**, 64–72.

Helmholtz, H. von (1853) Über einige Gesetze der Verteilung elektrischer Ströme in körperlichen Leitern, mit Anwendung auf die thierisch–elektrischen Versuche. *Ann. Phys. Chem.*, **89**, 211–233, 353–377.

Hoenig, H.E., Daalmans, G.M., Bär, L., Bömmel, F., Paulus, A., Uhl, D., Weisse, H.J., Schneider, S., Seifert, H., Reichenberger, H. and Abraham-Fuchs, K. (1991) Multichannel DC SQUID sensor array for biomagnetic applications. *IEEE Trans. Magn.*, **27**, 2777–2785.

Hoke, M. (1988) SQUID-based measuring techniques—a challenge for the functional diagnostics in medicine. In Kramer, B. (ed.), *The Art of Measurement: Metrology in Fundamental and Applied Physics*. VCH Verlagsgesellschaft, Weinheim, pp. 287–335.

Hummel, T. and Kobal, G. (1992) Differences in human evoked potentials related to olfactory or trigeminal chemosensory activation. *Electroenceph. Clin. Neurophysiol.*, 84, 84–89.

Hummel, T., Pauli, E., Schüler, P., Kettenmann, B., Stefan H. and Kobal, G. (1995) Chemosensory event-related potentials in patients with temporal lobe epilepsy. *Epilepsia*, **26**, 79–85.

Janday, B.S. and Swithenby, S.J. (1987) Analysis of magneto-encephalographic data using the homogeneous sphere model: empirical tests. *Phys. Med. Biol.*, **32**, 105–113.

Kettenmann, B., Jousmäki, V., Portin, K., Salmelin, R., Kobal, G. and Hari, R. (1996) Odorants activate the human superior temporal sulcus. *Neurosci. Lett.*, **203**, 1–3.

Kobal, G. (1981) *Elektrophysiologische Untersuchungen des menschlichen Geruchssinns*. Thieme, Stuttgart, p. 171.

Kobal, G. (1985) Pain-related electrical potentials of the human nasal mucosa elicited by chemical stimulation. *Pain*, **22**, 151–163.

Kobal, G. and Hummel, T. (1988) Olfaction: chemosensory evoked potentials in patients with olfactory disturbances. *Rhinology*, **26**(suppl.), 1–18.

Kobal, G. and Hummel, T. (1991) Olfactory evoked potentials in humans. In Getchell, T.V., Doty, R.L., Bartoshuk, L.M. and Snow, J.R., Jr (eds), *Smell and Taste in Health and Disease*. Raven Press, New York, pp. 255–275.

Kobal, G. and Plattig, K.-H. (1978) Methodische Anmerkungen zur Gewinnung olfaktorischer EEG—Antworten des wachen Menschen (objektieve olfaktometrie). *Z. EEG–EMG*, **9**, 135–145.

Kobal, G., Van Toller, S. and Hummel T. (1989) Is there directional smelling? *Experientia*, **45**, 130–132.

Kobal, G., Hummel, T. and Van Toller, S. (1992) Differences in human chemosensory evoked potentials to olfactory and somatosensory chemical stimuli presented to left and right nostrils. *Chem. Senses*, **17**, 233–244.

Koizuka, I., Yano, H., Nagahara, M., Seo, R., Shimada, K., Kubo, T. and Nogawa, T. (1994) Functional imaging of the human olfactory cortex by magnetic resonance imaging. *ORL*, **56**, 273–275.

Livermore, A., Hummel, T. and Kobal, G. (1992) Chemosensory evoked potentials in the investigation of interactions between the olfactory and the somatosensory (trigeminal) system. *Electroenceph. Clin. Neurophysiol.*, **83**, 201–210.

Marquardt, D.W. (1963) An algorithm for least-squares estimation of nonlinear parameters. *J. Soc. Ind. Appl. Math.*, **11**, 431–441.

Meijs, J.W., ten Voorde, B.J. and Peters, J.M. (1988) On the influence of various head models on EEGs and MEGs. In Pfurtscheller, G., Lopes da Silva, F.H. (eds), *Functional Brain Imaging*. Springer Verlag, Berlin, pp. 31–45.

Mesulam, M.-M. and Mufson, E.J. (1982) Insula of the old world monkey. I. Architectonics in the insulo-orbito-temporal component of the paralimbic brain. *J. Comp. Neurol.*, **212**, 1–22.

Murphy, C. (1987) olfactory psychophysics. In: *Neurobiology of Taste and Smell*. Wiley, New York, 251–274.

Price, J.L. (1990) Olfactory system. In Paxinos, G. (ed.), *The Human Nervous System*. Academic Press, San Diego, CA, pp. 979–998.

Powell, M.J.D. (1964) An efficient method for finding the minimum of a function of several variables without calculating derivatives. *Comput. J.*, **7**, 155–162.

Romani, G.L., Williamson, S.J. and Kaufman, L. (1982) Biomagnetic instrumentation. *Rev. Sci. Instrum.*, **53**, 1815–1845.

Romani, G.L. and Narici, L. (1986) Principles and clinical validity of the biomagnetic method. *Med. Progr. Technol.*, **11**, 123–159.

Scholz, B. and Oppelt, A. (1992) Probability based dipole localization and individual localization error calculation in biomagnetism. *Proc. Ann. IEEE Med. Biol. Soc.*, **14**, 1766–7.

Silver, W.L., Mason, J.R., Marshall, D.A. and Maruniak, J.A. (1986) Rat trigeminal, olfactory and taste responses after capsaicin desensitization. *Brain Res.*, **333**, 45–54.

Stefan, H., Schneider, S., Abraham, K., Bauer, J., Neubauer, U., Röhrlein, G. and Huk, W.J. (1990) Magnetic source localization in focal epilepsy; first experiences with multichannel MEG correlated to MR brain imaging. *Brain*, **113**, 1347–1359.

Williamson, S.J. and Kaufman, L. (1981) Biomagnetism. *J. Magn. Magn. Mat.*, **22**, 129–201.

Williamson, S.J. and Kaufman, L. (1989) Advances in neuromagnetic instrumentation and studies of spontaneous brain activity. *Brain Topogr.*, **2**, 129–139.

Youngentoub, S.L., Kurtz, D.B., Leopold, D.A., Mozell, M.M. and Hornung, D.E. (1982) Olfactory sensitivity: is there laterality? *Chem. Senses*, **7**, 1–9.

Zatorre, R.J., Jones-Gotman, M., Evans, A.C. and Meyer, E. (1992) Functional localization and lateralization of human olfactory cortex. *Nature*, **360**, 339–340.

Received on May 14, 1996; accepted on May 8, 1997